NEW SCALING LAWS IN ZPG TURBULENT BOUNDARY LAYER FLOW

George Khujadze & Martin Oberlack
Fluid Dynamics Group,
Department of Mechanical Engineering,
Technische Universität Darmstadt,
Hochschulstr. 1, 64289, Darmstadt, Germany
khujadze@fdy.tu-darmstadt.de & oberlack@fdy.tu-darmstadt.de

ABSTRACT

Lie group or symmetry approach applied to turbulence as developed by Oberlack (see e.g. Oberlack (2001) and references therein) is used to derive *new scaling laws* for various statistical quantities of a zero pressure gradient (ZPG) turbulent boundary layer flow. From the two-point correlation (TPC) equations the knowledge of the symmetries allows us to derive a variety of invariant solutions (scaling laws) for turbulent flows, one of which is the new exponential mean velocity profile that is found in the mid-wake region of flat-plate boundary layers. Further, a third scaling group was found in the TPC equations for the one-dimensional turbulent boundary layer. This is in contrast to the Navier-Stokes and Euler equations which has one and two scaling groups respectively.

LIE GROUP ANALYSIS OF TPC EQUATIONS

Lie group analysis was applied to the TPC equations to find their symmetry groups and thereof to derive invariant solutions (scaling laws). The present analysis is based on TPC equations under the assumption of a parallel mean velocity profile $\bar{u}_i \equiv [\bar{u}_1(x_2), 0, 0]$ (where x_2 is the wall normal coordinate) and sufficiently apart from the viscous sublayer we have

$$\left(\frac{\partial}{\partial t} + \bar{u}_k \frac{\partial}{\partial x_k}\right) R_{ij} + R_{kj}\frac{\partial \bar{u}_i}{\partial x_k} + R_{ik}\frac{\partial \bar{u}_j}{\partial x_k}\bigg|_{\boldsymbol{x}+\boldsymbol{r}} + [\bar{u}_k(\boldsymbol{x}+\boldsymbol{r}) - \bar{u}_k(\boldsymbol{x})]\frac{\partial R_{ij}}{\partial r_k} + \frac{\partial \overline{p'u'}_j}{\partial x_i} - \frac{\partial \overline{p'u'}_j}{\partial r_i} + \frac{\partial \overline{u_i'p'}}{\partial r_j} + \frac{\partial R_{(ik)j}}{\partial x_k} - \frac{\partial}{\partial r_k}[R_{(ik)j} - R_{i(jk)}] = 0 \tag{1}$$

where

$$\begin{aligned} R_{ij} &= \overline{u_i'(\boldsymbol{x},t)u_j'(\boldsymbol{x}+\boldsymbol{r})} \\ \overline{p'u_j'} &= \overline{p'(\boldsymbol{x})u_j'(\boldsymbol{x}+\boldsymbol{r})} \\ \overline{u_i'p'} &= \overline{u_i'(\boldsymbol{x})p'(\boldsymbol{x}+\boldsymbol{r})} \\ R_{(ik)j} &= \overline{u_i'(\boldsymbol{x})u_k'(\mathbf{x})u_j'(\boldsymbol{x}+\boldsymbol{r})} \\ R_{i(jk)} &= \overline{u_i'(\boldsymbol{x}+\boldsymbol{r})u_j'(\mathbf{x})u_k'(\boldsymbol{x})} \end{aligned} \tag{2}$$

are two- and three-point correlation functions. Pressure-velocity correlations are determined by the Poisson equation and hence they are not independent of the velocity correlations. The only unclosed terms in the equation are triple correlations.

Lie's procedure to find symmetry transformations and the derivation of self-similar solutions may be divided into three parts. The first one, the computation of the "determining system", is completely algorithmic (this is one of the important advantages of the method) and has been aided by the Lie group software package by Carminati and Vu (2000). The package is written for the computer algebra system (CAS) MAPLE. It computes the system of "determining equations", which consist of a coupled, linear, homogeneous and overdetermined system of partial differential equations for the infinitesimals. In the first step of the present approach the infinitesimal generators must be determined from equation (1). As a result, an over-determined set of ~ 700 linear partial differential equations are obtained. The full solution of the "determining equations", i.e. the second step of Lie's procedure, is given in Khujadze (2006).

For the present problem we focus only on the scaling symmetries, Galilean invariance and the translation groups. For all latter groups the generators may be written as:

$$\begin{aligned} X_1 &= x_2\frac{\partial}{\partial x_2} + r_i\frac{\partial}{\partial r_i} + \bar{u}_1\frac{\partial}{\partial \bar{u}_1} + 2R_{ij}\frac{\partial}{\partial R_{ij}} + 3\overline{u_i'p'}\frac{\partial}{\partial \overline{u_i'p'}} + 3\overline{p'u'}_i\frac{\partial}{\partial \overline{p'u'}_i}\cdots \\ X_2 &= -\bar{u}_1\frac{\partial}{\partial \bar{u}_1} - 2R_{ij}\frac{\partial}{\partial R_{ij}} - 3\overline{u_i'p'}\frac{\partial}{\partial \overline{u_i'p'}} - 3\overline{p'u_i'}\frac{\partial}{\partial \overline{p'u_i'}} \\ X_3 &= R_{ij}\frac{\partial}{\partial R_{ij}} + \overline{u_i'p_i'}\frac{\partial}{\partial \overline{u_i'p_i'}} + \overline{p_i'u_i'}\frac{\partial}{\partial \overline{p_i'u_i'}} + \cdots \\ X_4 &= \frac{\partial}{\partial x_2} \\ X_5 &= \frac{\partial}{\partial \bar{u}_1} \end{aligned} \tag{3}$$

Employing Lie's differential equations (see Olver 1993), the global transformations for all groups are given by

$$\boldsymbol{G}_{s1}: \tilde{x}_2 = x_2 e^{c_1},\ \tilde{r}_i = r_i e^{c_1}, \tilde{\bar{u}}_1 = \bar{u}_1 e^{c_1},$$
$$\tilde{R}_{ij} = R_{ij}e^{2c_1}, \widetilde{\overline{p'u_i'}} = \overline{p'u_i'}e^{3c_1},\ \widetilde{\overline{u_i'p'}} = \overline{u_i'p'}e^{3c_1}, \cdots$$

$$\boldsymbol{G}_{s2}: \tilde{x}_2 = x_2,\ \tilde{r}_i = r_i,\ \tilde{\bar{u}}_1 = \bar{u}_1 e^{-c_2},$$
$$\tilde{R}_{ij} = R_{ij}e^{-2c_2}, \widetilde{\overline{p'u_i'}} = \overline{p'u_i'}e^{-3c_2},\ \widetilde{\overline{u_i'p'}} = \overline{u_i'p'}e^{-3c_2}, \cdots$$

$$\boldsymbol{G}_{s3}: \tilde{x}_2 = x_2,\ \ \tilde{r}_i = r_i,\ \ \tilde{\bar{u}}_1 = \bar{u}_1,$$
$$\tilde{R}_{ij} = R_{ij}e^{-c_3},\ \ \widetilde{\overline{p'u_i'}} = \overline{p'u_i'}e^{-c_3},\ \ \widetilde{\overline{u_i'p'}} = \overline{u_i'p'}e^{-c_3}, \cdots$$

$$\boldsymbol{G}_{transl}: \tilde{x}_2 = x_2 + c_4,\ \ \tilde{r}_i = r_i,\ \ \tilde{\bar{u}}_1 = \bar{u}_1,$$
$$\tilde{R}_{ij} = R_{ij},\ \ \widetilde{\overline{p'u_i'}} = \overline{p'u_i'},\ \ \widetilde{\overline{u_i'p'}} = \overline{u_i'p'}, \cdots$$

$$\boldsymbol{G}_{galil}: \tilde{x}_2 = x_2,\ \ \tilde{r}_i = r_i,\ \ \tilde{\bar{u}}_1 = \bar{u}_1 + c_5,$$
$$\tilde{R}_{ij} = R_{ij}, \widetilde{\overline{p'u_i'}} = \overline{p'u_i'},\ \ \widetilde{\overline{u_i'p'}} = \overline{u_i'p'}, \cdots \tag{4}$$

The variables $c_1 - c_5$ are the group parameters of the corresponding transformations. The dots denote that also higher order correlations are involved in the corresponding symmetry.

The most interesting fact with respect to the latter groups is that *three independent scaling groups* $\boldsymbol{G}_{s1}$, $\boldsymbol{G}_{s2}$, $\boldsymbol{G}_{s3}$ have been computed. Two symmetry groups correspond to the scaling symmetries of the Euler equations. The first one is the scaling in space, the second one scaling in time. The third group (G_{s3}) is a new scaling group that is a characteristic feature only of the one-dimensional turbulent boundary layer flow. It is a new scaling symmetry not obtained before. This is in striking contrast to the Euler and Navier-Stokes equations, which only admit two and one scaling groups, respectively. $\boldsymbol{G}_{transl}$ and $\boldsymbol{G}_{galil}$ represent the translation symmetry in space and the Galilean transformation, respectively.

The corresponding characteristic equations for the invariant solutions (Oberlack 2001) read

$$\frac{dx_2}{c_1x_2+c_4} = \frac{dr_i}{c_1r_i} = \frac{d\bar{u}_1}{(c_1-c_2)\bar{u}_1+c_5} = \frac{dR_{ij}}{[2(c_1-c_2)+c_3]R_{ij}} = \frac{d\overline{p'u_i'}}{[3(c_1-c_2)+c_3]\overline{p'u_i'}} = \cdots \tag{5}$$

In Oberlack (2001) it has been shown that the symmetry breaking of the scaling of space leads to a new exponential scaling law. Therein it was argued that physically it corresponds to the outer part of a boundary layer flow, the wake region. Thus, invoking the symmetry breaking constraint of an external length scale ($c_1 = 0$) the exponential scaling law for the wake region of a ZPG turbulent boundary layer flow has been obtained and further validated, e.g. in Khujadze and Oberlack (2004). The characteristic equation for the velocity will reduce to the following form:

$$\frac{dx_2}{c_4} = \frac{d\bar{u}_1}{-c_2\bar{u}_1+c_5} \tag{6}$$

Integrating this equation we obtain scaling law for the mean velocity as follows:

$$\bar{u}_1(x_2) = k_1 + k_2 e^{-k_3 x_2}, \tag{7}$$

where

$$k_1 \equiv \frac{c_5}{c_2}, \qquad k_3 \equiv \frac{c_2}{c_4}$$

and k_2 is a constant of integration.

For positive k_3 the velocity law (7) converges to a constant velocity for $x_2 \to \infty$ ($k_1 = \bar{u}_\infty$). For a plane shear flow this may only be applicable to a boundary layer type of flow. In this flow the symmetry breaking length scale is the boundary layer thickness.

As for the TPC functions R_{ij} we have the equation:

$$\frac{dx_2}{c_4} = \frac{dR_{ij}}{(-2c_2+c_3)R_{ij}} \tag{8}$$

The solution of this equation gives the following:

$$R_{ij}(x_2, \boldsymbol{r}) = e^{-k_4 x_2} B_{ij}(\boldsymbol{r}) \tag{9}$$

Besided the latter we obtained the following scaling laws also for the mean values and the TPC pressure-velocity functions:

$$\frac{\bar{u}_\infty - \bar{u}_1}{u_\tau} = \alpha \exp\left(-\beta \frac{x_2}{\Delta}\right) \tag{10}$$

$$\overline{u_i'p'}(x_2, \boldsymbol{r}) = e^{-(k_3+k_4)x_2} E_i(\boldsymbol{r}) \tag{11}$$

	Re_θ	$N_{max} \times 10^6$	$\Delta x_1^+, \Delta x_2^+, \Delta x_3^+$
$N1$	810	31.2	$16, 0.04-5, 5.5$
$N2$	2240	138.9	$15, 0.06-5, 11$
$N3$	2800	538	$11, 0.06-5, 10$

Table 1: Parameters of performed simulations.

$$\overline{p'u_i'}(x_2, \boldsymbol{r}) = e^{-(k_3+k_4)x_2} F_i(\boldsymbol{r}) \tag{12}$$

where α, β, k_3, k_4 are universal constants and B_{ij}, E_i, F_i are only a function of the correlation distance $\boldsymbol{r}$. From the equation (9) we may deduce two important results:

- In non-dimensional form the Reynolds stresses have the form:
$$\frac{\overline{u_i'u_j'}(x_2)}{u_\tau^2} = b_{ij} \exp\left(-a\frac{x_2}{\Delta}\right) \tag{13}$$
- The TPC correlation may be reduced to the correlation coefficient using (13) and (9):
$$\mathcal{R}_{[ij]}(\boldsymbol{r}) \equiv \frac{R_{ij}(x_2, \boldsymbol{r})}{\overline{u_i'u_j'}(x_2)} = B'_{[ij]}(\boldsymbol{r}) \tag{14}$$

where u_τ is the friction velocity; b_{ij} are the non-dimensional Reynolds stresses and a is a parameter independent of 'i' and 'j'; $B'_{[ij]}$ is independent of x_2; Δ is the Rotta-Clauser length-scale:

$$\Delta \equiv \int_0^\infty \frac{\bar{u}_\infty - \bar{u}_1}{u_\tau} dx_2 = \frac{\bar{u}_\infty}{u_\tau}\delta^*$$

while δ^* is the boundary layer displacement thickness:

$$\delta^*(x_1) \equiv \int_0^\infty \left(1 - \frac{\bar{u}_1}{\bar{u}_\infty}\right) dx_2 \tag{15}$$

The classical theory of turbulent boundary layer flow leads to the classical log-law in the overlap region which has the following form in the inner variables:

$$\bar{u}_1(x_2)^+ = \frac{1}{\kappa} ln(x_2^+) + B \tag{16}$$

where κ and B are constants that have to be found from experiments and/or DNS.

Here we would like to repeat the derivation of the log-law from Lie group analysis performed first by Oberlack (2001). In the equation (5) the assumption $c_1 = c_2$ leads to the following ordinary differential equation:

$$\frac{dx_2}{c_1x_2+c_4} = \frac{d\bar{u}_1}{c_5} \tag{17}$$

The solution of this equation is:

$$\bar{u}_1 = \frac{c_5}{c_1} ln(c_1x_2 + c_4) + C_1 \tag{18}$$

where C_1 is the integration constant. c_1, c_4, c_5 are group constants. This equation can be rewritten in the following form using inner scaling:

$$\bar{u}_1(x_2)^+ = \frac{1}{\kappa} ln(x_2^+ + A^+) + B \tag{19}$$

where A^+ is the additional constant in the logarithm.

NUMERICAL SIMULATIONS

For the verification of the new scaling laws a direct numerical simulations (DNS) at $Re_\theta = 810, 2240, 2800$, where

θ is the momentum loss thickness (see equation 20) were performed (for details see the table 1) using a spectral method with up to 538 million grid points (Khujadze and Oberlack 2004).

$$\theta(x_1) \equiv \int_0^\infty \frac{\bar{u}_1}{\bar{u}_\infty}\left(1 - \frac{\bar{u}_1}{\bar{u}_\infty}\right) dx_2 \qquad (20)$$

The code for the DNS was developed at KTH, Stockholm (Lundbladh et al. 1999). The main aim of the simulations were to validate the new exponential laws for mean velocity profile, Reynolds stresses and TPC functions.

The simulations for the low Reynolds number case were run for a total of 35000 time units ($\delta^*/\bar{u}_\infty$, where $\bar{u}_\infty$ is the freestream velocity) and the sampling for the statistics was performed during the last 30000 time units. The simulations at higher Reynolds numbers were run for $10000\delta^*/\bar{u}_\infty$ time units. The statistical averaging was performed during the last 8000 time units. The simulation times for latter cases were smaller because of the high computer resources required in these cases. However, the simulation time was in each cases enough to get smooth statistics.

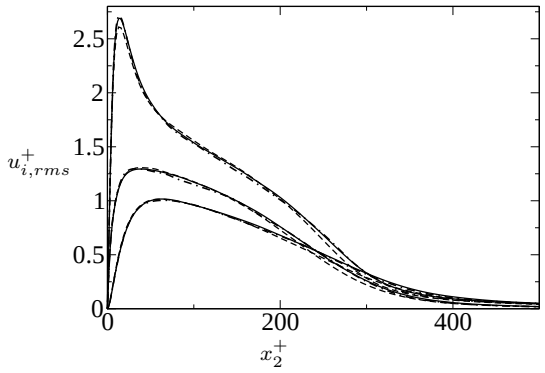

Figure 1: $u^+_{i,rms}$: − − − 7.9 (480 × 129 × 128), —— 31.2 (800 × 217 × 180) and —·— 74 (800 × 361 × 280) million grid points at $Re_\theta = 810$.

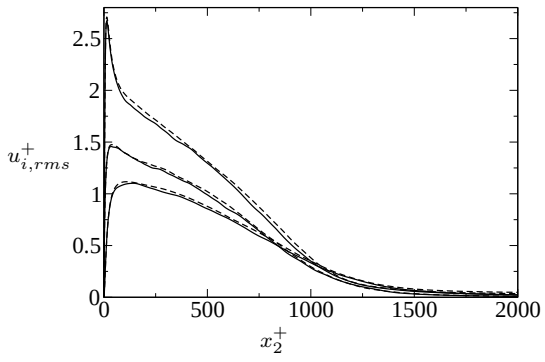

Figure 2: $u^+_{i,rms}$: —— 269 (2048 × 513 × 256) and − − − 538 (4096 × 513 × 256) million grid points at $Re_\theta = 2800$.

We would like to give briefly the results of performed DNS. The comparison between different resolutions at the same Reynolds numbers (for $u_{i,rms}$) is shown in Figs. 1 and 2. The difference between them is small even though the number of points in each direction for the coarser grid is reduced by a factor of 2. Fig. 1 shows resolution comparison at $Re_\theta = 810$ for three different number of grid points, beginning from ≈ 8 up to ≈ 74 million. As we see there is no big difference between the cases and curves collapse into one. The same picture is observed for the highest Reynolds number in Fig. 2. In the latter case the useful region was confined to $100 - 300\delta^*|_{x=0}$ (total length of computational box is $450\delta^*|_{x=0}$, where $\delta^*|_{x=0}$ is the thickness of laminar boundary layer flow) which corresponds to Re_θ from 1850 to 2800.

DNS for Reynolds number $Re_\theta = 2800$ was done with two different resolutions (see Fig. 2): $N \approx 270$ and 538 million grid points (2048 × 513 × 256 and 4096 × 513 × 256). The jobs were run on the Hitachi supercomputer in Munich (MPI version of the code) on 256 and on the IBM supercomputer using 128 CPUs (OpenMP version of the code) at TU Darmstadt.

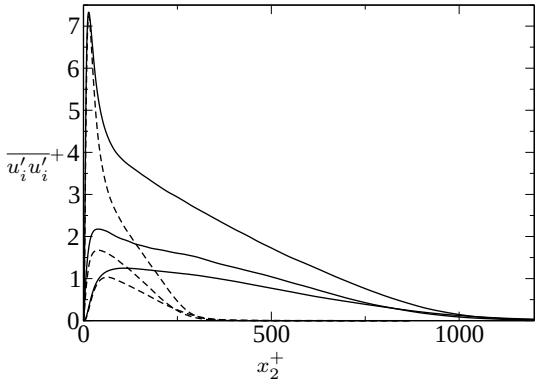

Figure 3: Reynolds stresses $\overline{u_i'u_i'}^+$ for different Reynolds numbers: − − − $Re_\theta = 810$; —— $Re_\theta = 2800$.

The comparison of Reynolds stress diagonal components are shown in the Fig. 3 in plus units at $Re_\theta = 810, 2800$.

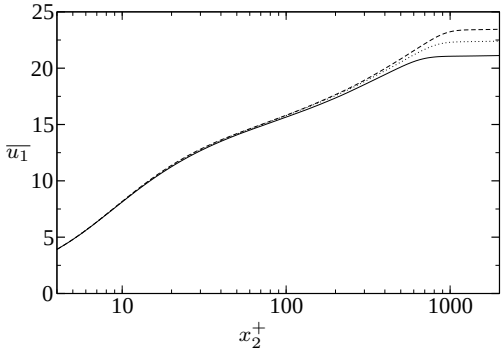

Figure 4: mean velocity profilesat different Reynolds numbers: —— $Re_\theta = 1850$; ····· $Re_\theta = 2330$; $Re_\theta = 2800$.

Fig. 4 displays mean velocity profiles from the last simulation ($Re_\theta = 2800$) taken at different places of the simulations box.

VERIFICATION OF THE SCALING LAWS

Exponential law

The mean velocity of the turbulent boundary layer data is plotted in Fig. 5 for $Re_\theta = 2240$ in outer scalings. As one can see from the figure, DNS and the theoretical result (equation 10) are in good agreement in the region $x_2/\Delta \approx 0.01 - 0.15$.

Using DNS we can find the constants in equation (13):

$$\begin{aligned} \overline{u_1'u_1'}(x_2) &= 4.55e^{-7.2x_2} \\ \overline{u_2'u_2'}(x_2) &= 2.7e^{-7.2x_2} \\ \overline{u_3'u_3'}(x_2) &= 1.8e^{-7.2x_2} \end{aligned} \qquad (21)$$

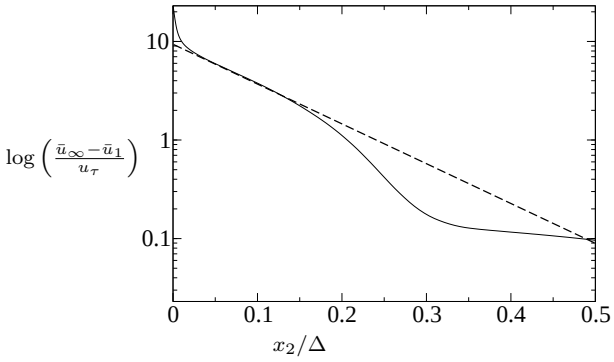

Figure 5: Mean velocity profile in log-linear scaling. – – – theoretical result from the law (10). —— DNS results for the simulation.

Fig. 6 shows the comparison of the theoretical result (13) with the DNS data in log-linear scaling at $Re_\theta = 810$. The key result is that the constant in the exponent is the same ($a = 7.2$) for all components of Reynolds stress tensor as it follows from the equation (13). This is expressed by the parallel dashed lines in Fig. 6 for the three normal stresses.

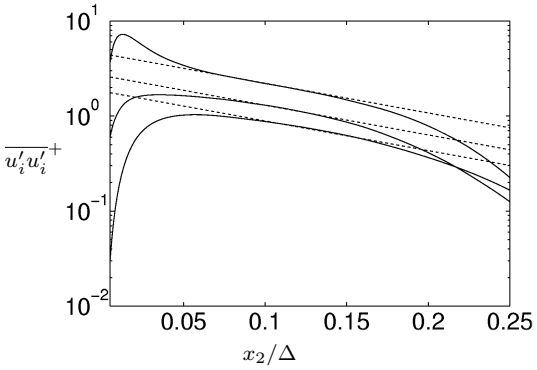

Figure 6: Reynolds stresses in log-linear scaling. Upper, lower and middle curves are $\overline{u_1' u_1'}$, $\overline{u_2' u_2'}$, $\overline{u_3' u_3'}$ respectively. – – – theoretical results (21). —— DNS results at $Re_\theta = 810$.

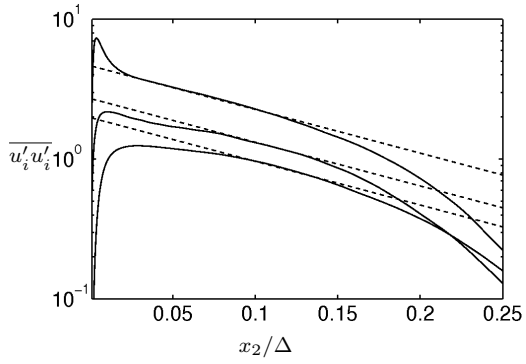

Figure 7: The same as in Fig. 6 but at $Re_\theta = 2800$.

The curves of equation (13) are shown in Fig. 7 comparing them to the DNS results at $Re_\theta = 2800$. We see that the results are in very good agreement.

The next result is shown in Fig. 8 when the plot of $\overline{u_1' u_1'}$ is shown at $Re_\theta = 810, 2240$. The exponential region increases towards the wall as the Reynolds number increases.

In Fig. 9 the mean velocity profile is shown with exponential and log regions at low Reynolds number. The constants in the equation (13) are: $\alpha = 9.4$ and $\beta = 9.0$. As for the log-law we found that $\kappa = 0.38$ and $C = 3.7$.

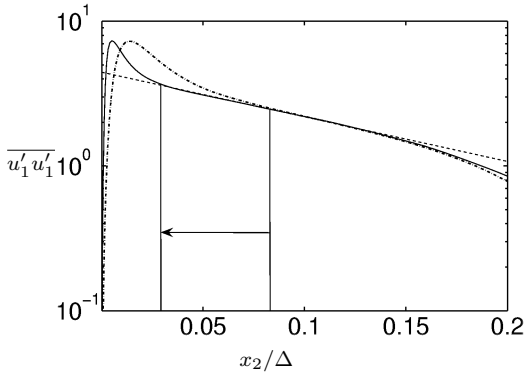

Figure 8: $\overline{u_1' u_1'}$ at —·— $Re_\theta = 810$, —— $Re_\theta = 2240$ Reynolds numbers.

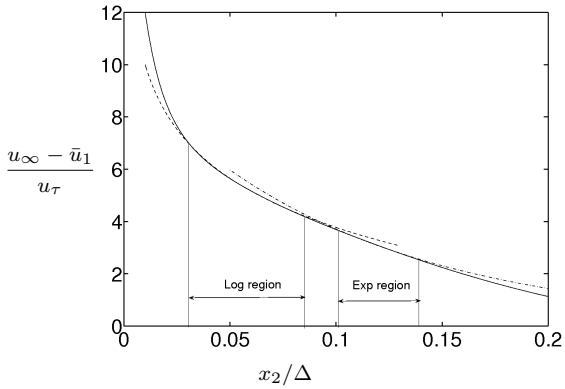

Figure 9: Mean velocity profile for at $Re_\theta = 1015$. —— log-law, – – – DNS, —·— exponential law.

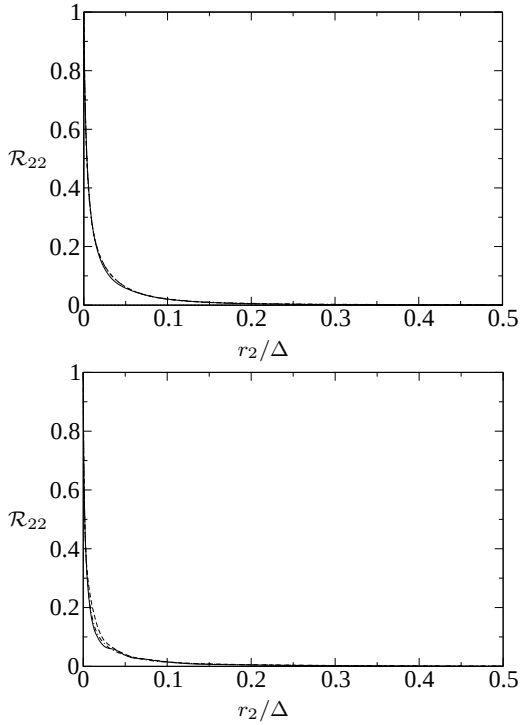

Figure 10: Correlation coefficient $\mathcal{R}_{22}$. *Top plot:* $Re_\theta = 810$. $x_2/\Delta = 0.1, 0.12, 0.13, 0.144$; *Bottom plot:* $Re_\theta = 2240$. $x_2/\Delta = 0.095, 0.126, 0.16$.

The second important result is the verification of equation (14). The correlation coefficient in the case of ZPG turbulent boundary layer flow (in the parallel flow approximation) has the following form:

$$\mathcal{R}_{[22]} = \frac{\overline{u_2'(x_2,t)u_2'(x_2+r_2)}}{\overline{u_2'u_2'}(x_2)} \tag{22}$$

Equation (22) is verified in Fig. 10: top plot corresponds to Reynolds number $Re_\theta = 810$. TPC coefficients are plotted at the different initial points $x_2/\Delta = 0.1, 0.12, 0.13, 0.144$ are located in the exponential region of the flow; Bottom plot corresponds to $Re_\theta = 2240$ with $x_2/\Delta = 0.095, 0.126, 0.16$. In both cases the lines collapse in one, that means that the correlation coefficients are independent of the wall distance x_2 as it was suggested by the equation (14).

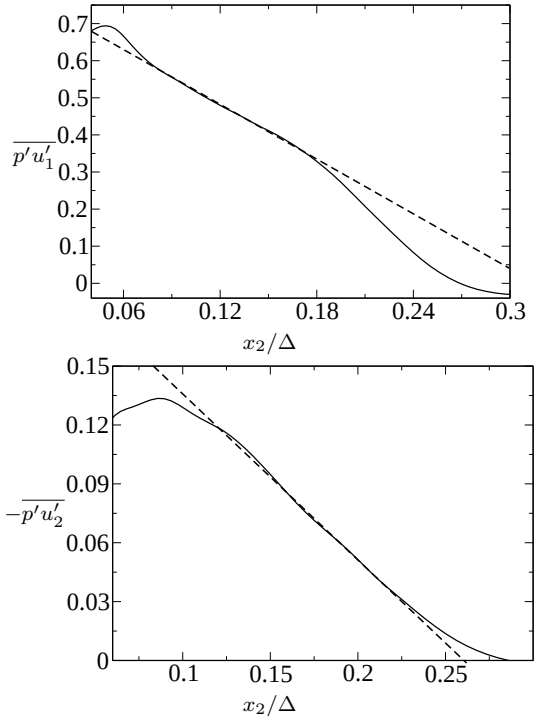

Figure 11: Pressure velocity correlations —— DNS ($Re_\theta = 810$), – – – theoretical result. Left figure: $\overline{p'u_1'}$; Right figure: $-\overline{p'u_2'}$;

In Fig. 11 DNS results are compared to the theoretical ones for the pressure-velocity correlations. The exponential region for $\overline{p'u_1'}$ is $x_2/\Delta \approx 0.04-0.18$, while the law for $-\overline{p'u_2'}$ is valid in the interval of $x_2/\Delta \approx 0.15 - 0.22$.

Modified log-law

In a recent paper by Österlund et al. (2000) the authors performed two independent experimental investigations of the behavior of turbulent boundary layers with different Reynolds numbers $Re_\theta = 2500 - 27000$. The experiments were performed in two facilities, the minimum turbulence level wind tunnel at Royal Institute of Technology (KTH) and the National Diagnostic Facility wind tunnel at Illinois Institute of Technology. The aim of the experiments was to understand the characteristics of the overlap region between inner and outer region of the boundary layer flow. They state that no significant Reynolds number dependence for the parameters describing the overlap region using the classical logarithmic relation were found and that the data analysis shows the viscous influence to extend within the buffer layer up to $x_2^+ \approx 200$ instead of the previously assumed value $x_2^+ \approx 50$. The parameters of the log-law are constant: $\kappa = 0.38, B = 4.1$. The authors explain the result with the low Reynolds number effects in previous experiments.

Equation (19) has an additional constant A^+ in the logarithmic function in comparison to the classical one.

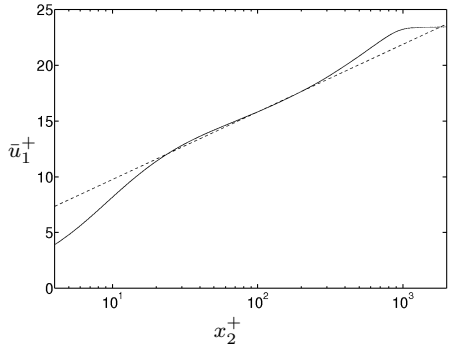

Figure 12: Mean velocity profile in inner scaling at $Re_\theta = 2500$. —— experiments and DNS data; – – – theoretical results (equation (16)).

The classical log-law is compared to the DNS at $Re_\theta = 2800$ in Fig. 12. The constants for the log-law are: $\kappa = 0.38$ and $B = 3.7$.

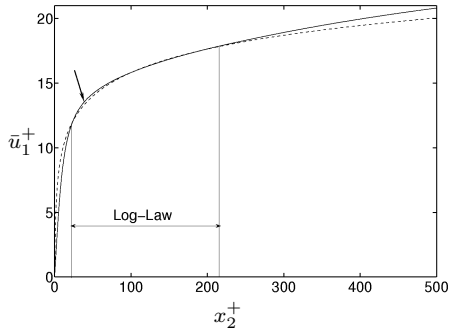

Figure 13: Mean velocity profile in inner scaling at $Re_\theta = 2800$. Parameters from Fig. 12.

In Fig. 13 the same velocity profile is shown but in normal scaling. The logarithmic region is located in the range of $x_2^+ \approx 30 - 220$.

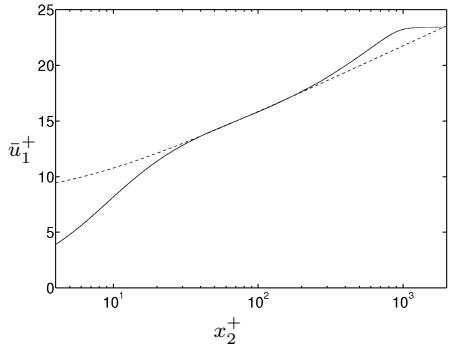

Figure 14: Mean velocity profile in inner scaling at $Re_\theta = 2800$ for the modified log-law. —— experiments and DNS data; – – – theoretical results (equation 19)

Figs. 14 and 15 show mean velocity profile for modified log-law (see equation (19)) for log and normal scaling. The

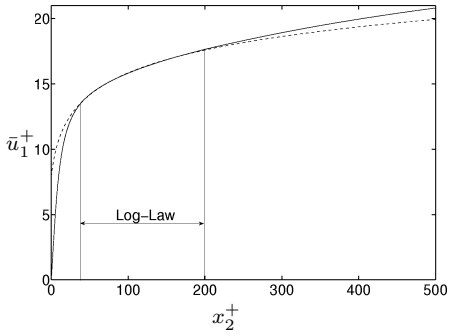

Figure 15: Mean velocity profile in inner scaling. Parameters from Fig. 14.

constants for the logarithmic law are: $\kappa = 0.383$, $B = 3.7$ and $A^+ = 5$. As it is seen from these figures, the log-region extends in comparison with the classical log-law.

Comparison of Figs. 12, 13, 14 and 15 shows that the modified log-law better fits the DNS results. Namely in the region shown by an arrow in Fig. 13, where classical log-law does not fits perfectly with the DNS. The constants in the log-law are almost the same in both versions of the law.

SUMMARY

In the present work a Lie group analysis of the TPC equations is presented in the case of ZPG turbulent boundary layer flow using the parallel flow assumption ($\bar{u}_1 \equiv \bar{u}_1(x_2)$). It is shown that the Lie group analysis helps to gain more insight into the description of the turbulent flow. This method provides a systematical procedure to derive symmetries from a set of differential equations. The following results were obtained:

- The new exponential scaling law for the mean velocity profile, TPC functions, velocity-pressure correlations and Reynolds stresses were found in the mid-wake region of flat-plate boundary layers;
- A new, third scaling group $\boldsymbol{G}_{s3}$ (that is a characteristic feature only of the one-dimensional turbulent boundary layer flow) was found in the TPC equations in contrast to the Navier-Stokes and Euler equations which have one and two scaling groups, respectively.

Comparison of the DNS results to the theoretical ones is very promising:

- The exponential law exists for all statistical quantities as it was predicted by the Lie group analysis;
- Increase of the Reynolds number increases the region where this law is valid;
- DNS allows us to find the constants in the formula of the exponential laws;
- Statistics accumulation time is very important parameter for the validation of the exponential law.

ACKNOWLEDGEMENT

We would like to express the gratitude to Profs. Henningson and Johannson from KTH, Stockholm for given to us an opportunity the use their code for DNS developed in their groops.

REFERENCES

Carminati, J. and K. Vu (2000). Symbolic computation and differential equations: Lie symmetries. *J.Sym. Comp. 29*, 95–116.

Khujadze, G. (2006). *DNS and lie group analysis of zero pressure gradient turbulent boundary layer flow*. Thesis, Darmstadt, Techn. Univ.

Khujadze, G. and M. Oberlack (2004). Dns and scaling laws from new symmetry groups of zpg turbulent boundary layer flow. *TCFD 18*, 391–411.

Lundbladh, A., S. Berlin, M. Skote, C. Hildings, J. Choi, and K. D. Henningson (1999). The efficient spectral method for simulation of incompressible flow over a flat plate. Tech. rep., Royal Institute of Technology, Stokholm.

Oberlack, M. (2001). A unified approach for symmetries in plane parallel turbulent shear flows. *J. Fluid Mech. 427*, 299–328.

Olver, P. (1993). *Applications of Lie groups to Differential equations*, Volume 107 of *Graduate Texts in Mathematics*. Springer, New-York.

Österlund, J., A. Johansson, H. Nagib, and M. Hites (2000). A note on the overlap region in turbulent boundary layers. *Phys. Fluids 12*(1), 1–4.